

LMMCoDrive: Cooperative Driving with Large Multimodal Model

Haichao Liu, Ruoyu Yao, Zhenmin Huang, Shaojie Shen, and Jun Ma

Abstract—To address the intricate challenges of decentralized cooperative scheduling and motion planning in Autonomous Mobility-on-Demand (AMoD) systems, this paper introduces LMMCoDrive, a novel cooperative driving framework that leverages a Large Multimodal Model (LMM) to enhance traffic efficiency in dynamic urban environments. This framework seamlessly integrates scheduling and motion planning processes to ensure the effective operation of Cooperative Autonomous Vehicles (CAVs). The spatial relationship between CAVs and passenger requests is abstracted into a Bird’s-Eye View (BEV) to fully exploit the potential of the LMM. Besides, trajectories are cautiously refined for each CAV while ensuring collision avoidance through safety constraints. A decentralized optimization strategy, facilitated by the Alternating Direction Method of Multipliers (ADMM) within the LMM framework, is proposed to drive the graph evolution of CAVs. Simulation results demonstrate the pivotal role and significant impact of LMM in optimizing CAV scheduling and enhancing decentralized cooperative optimization process for each vehicle. This marks a substantial stride towards achieving practical, efficient, and safe AMoD systems that are poised to revolutionize urban transportation. The code is available at <https://github.com/henryhcliu/LMMCoDrive>.

I. INTRODUCTION

Autonomous Mobility-on-Demand (AMoD) Systems represent a transformative approach to urban transportation, which aim to efficiently and safely navigate complex urban environments to fulfill passenger requests with fleets of Cooperative Autonomous Vehicles (CAVs) [1]. These systems promise to revolutionize urban landscapes by mitigating traffic congestion, enhancing accessibility, and reducing transportation-related emissions. However, orchestrating such systems presents significant challenges, particularly in the realm of task scheduling and cooperative motion planning [2]. The inherent dynamic nature of AMoD systems necessitates continuous path adjustments for CAVs to manage both assigned and future tasks, thereby complicating vehicle scheduling in response to passenger requests within the intricate configurations of urban traffic systems [3].

Historically, research has been carried out to segregate the focus on scheduling, particularly on how CAVs are dispatched to meet user demands. Yet, the critical need for the integration of scheduling and motion planning is neglected. This separation overlooks the essential requirement for simultaneous motion planning and mutual avoid-

Haichao Liu and Ruoyu Yao are with the Robotics and Autonomous Systems Thrust, The Hong Kong University of Science and Technology (Guangzhou), China (e-mail: hliu369@connect.hkust-gz.edu.cn, ryao092@connect.hkust-gz.edu.cn).

Zhenmin Huang, Shaojie Shen and Jun Ma are with the Department of Electronic and Computer Engineering, The Hong Kong University of Science and Technology, Hong Kong SAR, China (e-mail: zhuangdf@connect.ust.hk; eeshaojie@ust.hk; jun.ma@ust.hk).

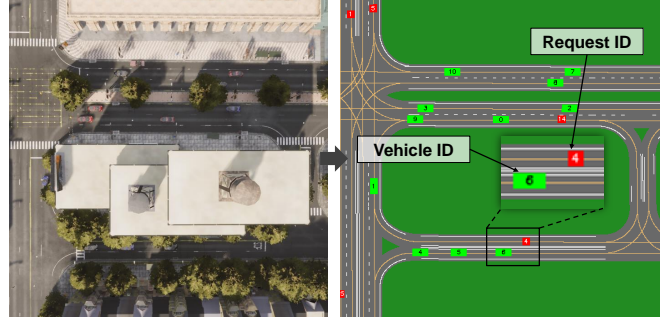


Fig. 1. Demonstration of the autonomous mobility-on-demand system in an urban scenario. The red squares denote the requests from passengers, while the free vehicles are supposed to be scheduled by the LMM. The abstracted bird-eye-view graphics are generated along with the supplementary textual information to be sent to the LMM for multiple decisions.

ance among assigned vehicles, which is crucial for the practical deployment of AMoD systems in complex urban environments. This research gap signifies a pressing need for possible integrated solutions.

The challenges of integrating intelligent scheduling with real-time cooperative motion planning for AMoD systems are threefold. First and foremost, there is the formidable challenge of developing a universally applicable scheduling strategy that can effectively navigate the intricacies of urban traffic systems, particular for rule-based and learning-based methods [4]. Secondly, ensuring an agile response from the motion planning level to changes at the scheduling level is essential for the dynamic urban traffic environment [5]. Lastly, achieving fast cooperative motion planning with a large number of CAVs, without compromising on safety or efficiency, introduces another level of complexity [6]. In light of these challenges, this work introduces LMMCoDrive, a novel approach leveraging a Large Multimodal Model (LMM) to enhance decentralized cooperative scheduling and motion planning of AMoD systems. Our primary contributions are as follows:

- We propose a novel LMM-enhanced framework that integrates scheduling and motion planning processes for CAVs, in which we leverage an informative BEV of the AMoD system to exploit the potential of LMMs in cooperative driving tasks.
- We present a decentralized optimization algorithm via the Alternating Direction Method of Multipliers (ADMM) under the guidance of LMM for graph evolution. It efficiently splits the CAVs into several sub-graphs, leading to smaller-sized OCPs for high compu-

tational efficiency.

- Experimental results demonstrate the effectiveness of LMMCoDrive in optimizing the scheduling of CAVs and also in the graph evolution process for the cooperative driving task. The results attained underscore a significant advancement for LMMs towards the realization of practical AMoD systems.

II. RELATED WORKS

A. Scheduling Methods for AMoD

Recent studies have delved into the application of Reinforcement Learning (RL) in the realm of scheduling for AMoD systems. For example, the integration of multi-agent Soft Actor-Critic with weighted bipartite matching achieves small-scale scheduling of the agents [7]. Despite their innovative strategies, RL-based methods grapple with inherent drawbacks. The complexity of AMoD scheduling, which encompasses numerous variables and scenarios, makes it challenging to define a clear and effective reward function [8]. Furthermore, the scarcity of real-world datasets for task scheduling of AMoD systems limits the practical applicability and training of RL models. To navigate the task allocation process, various rule-based methods have been proposed, such as Distance First (DF), Idle First (IF), and Priority First (PF) [9], [10]. These methods, guided by predefined rules, offer simplicity and interpretability but may lack the flexibility and scalability needed to address the inherent dynamic nature of urban transportation systems.

The advent of Large Language Model (LLM) has paved the way for advancements in task scheduling, owing to their prowess in open-world comprehension, reasoning, and few-shot acquisition of common sense knowledge [11]–[14]. Notable efforts like DiLu leverage textual descriptions of the environment for single-vehicle decision-making [15]. The potential of LLM to make contextual inferences and decisions heralds a promising direction for scheduling of AMoD systems. Nonetheless, the application of multimodal LLM or LMM in cooperative driving for AMoD systems has yet to be extensively explored [16]. With their information representation capabilities, especially in dealing with images, LMMs have the potential to greatly improve the depiction and comprehension of urban transportation systems, which could underscore a crucial research gap.

B. Cooperative Motion Planning Methods for AMoD

After the scheduling process of the AMoD system, each CAV is required to plan a feasible trajectory to be followed. Optimization-based approaches to cooperative motion planning typically employ a formulation as an Optimal Control Problem (OCP). This methodological framework offers a precise mathematical representation, strong interpretability, and guarantee of optimality [17], [18]. For CAVs with nonlinear vehicle models, OCPs are typically solved using established nonlinear programming solvers, such as interior point optimizer (IPOPT) and Sequential Quadratic Programming (SQP). Moreover, the iterative linear quadratic

regulator (iLQR) method, benefiting from Differential Dynamic Programming (DDP), addresses nonlinear optimization problems by retaining only the first-order term of dynamics through Gauss-Newton approximation [19]. However, traditional iLQR struggles to directly manage inequality constraints related to collision avoidance and physical limitations in this situation. To address this challenge, advanced variations such as control-limited DDP and constrained iLQR have been suitably developed [20]–[22].

To alleviate the computational burdens of cooperative driving in large-scale AMoD systems, ADMM emerges as a potent solution by decomposing the principal optimization problem into several sub-problems. Its parallel and distributed nature renders ADMM particularly suitable for cooperative motion planning of CAVs. For instance, dual consensus ADMM has been deployed to facilitate fully parallel optimization framework for cooperative motion planning of CAVs [23]. This approach significantly distributes computational efforts across all entities and attains real-time performance. Despite these advancements, existing methods fall short of supporting large-scale cooperative driving due to the fully connected nature of agents. Our prior research, which leverages the sparsity attribute of optimization problems for involved vehicles [24], indicates a promising pathway to enhance computational efficiency for AMoD systems, and this highlights another crucial research gap to be addressed.

III. PROBLEM FORMULATION

We consider a discrete-time system with N single-occupancy vehicles, denoted by \mathcal{V} . Customers randomly arrive and await transportation to their destinations. Unlike traditional first-come-first-serve (FCFS) methods, our system determines the order of service, prioritizing efficiency and directionality akin to ride-sharing practices.

The representation of CAVs' relationships using graph theory, where nodes and edges signify vehicles and communication links respectively, facilitates a detailed analysis of their interactions. We define an undirected graph $\mathcal{G} = (\mathcal{V}, \mathcal{E})$, with \mathcal{V} as the set of vehicles and \mathcal{E} as the communication links. Each vehicle $n^i \in \mathcal{V}$ has a state vector z^i and a control input vector u^i . Subgraphs \mathcal{H} , representing vehicle interactions within specific communication ranges, evolve over cooperative driving planning horizons. An edge $(n^i, n^j) = d^{i,j} \in \mathcal{E}_h \subseteq \mathcal{E}$ exists if the inter-vehicle distance $d^{i,j}$ is less than the communication range r_{tele}^i . The degree of a node n^i , i.e., $|n^i| = \deg(n^i)$, indicates its connectivity with the nodes in the set

$$\mathcal{N}^i = \{j \in \mathcal{N} \mid (i, j) \in \mathcal{E}_h\}. \quad (1)$$

This graph-theoretic model supports the development of scheduling and cooperative motion planning algorithms for AMoD systems.

IV. METHOD

Our proposed LMMCoDrive scheme mainly contains two parts: First, an LMM-based scheduling agent, is responsible

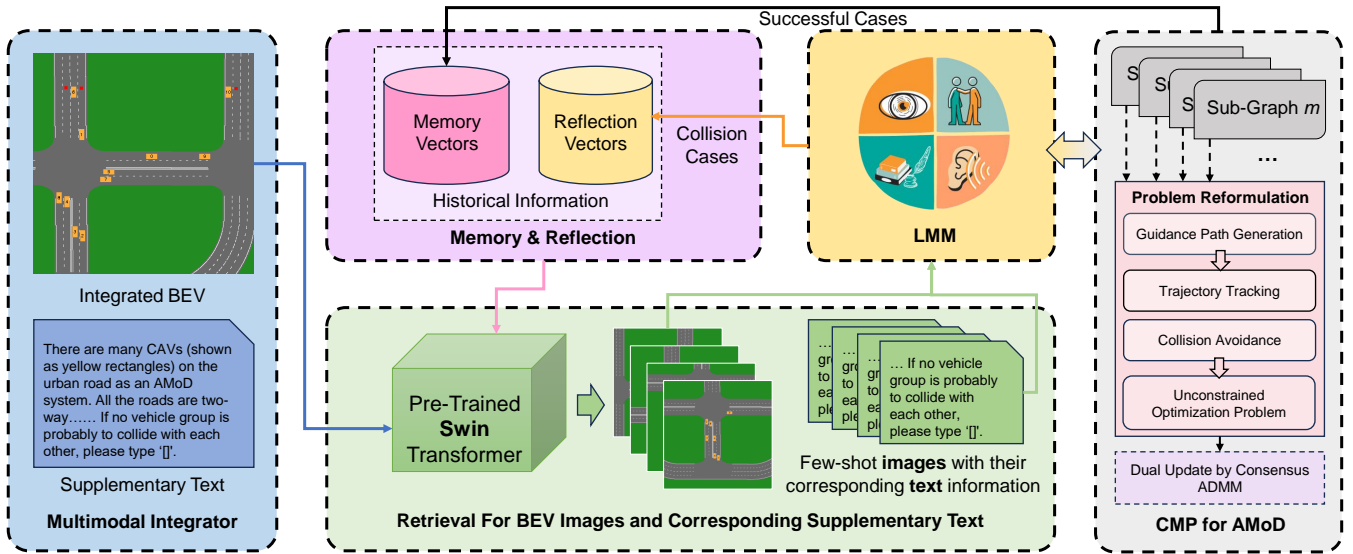


Fig. 2. Overall architecture of LMMCoDrive. It is composed of a multimodal integrator, a memory and reflection module, a retrieval module for similar memory and reflections, and a decentralized cooperative driving module. CMP means cooperative motion planning for the CAVs in the AMoD system.

for the multimodal information gathering, memory, reflection, and retrieval of similar historical situations. Second, an LMM-guided cooperative driving module, provides low-level motion planning for the vehicles and ensures the safety. The executing process is exhibited in Fig. 2.

A. LMM-Based Scheduling

The proposed LMM-based scheduling framework is designed to integrate and process multimodal information for effective task assignment of AMoD systems. This section delves into Information Integrator, Memory and Reflection Module, and Retrieval Module successively.

1) *Multimodal Integrator*: The multimodal integrator is pivotal in synthesizing data from various sources to generate a comprehensive understanding of the urban traffic environment and AMoD system status. This module comprises two primary components: BEV image generation and supplementary text generation.

This module starts by creating BEV images that encapsulate critical elements of the urban traffic landscape. These elements include road boundaries, lanes, CAVs each tagged with a unique ID, the centerlines of road lanes, and pending requests from passengers marked with unique IDs. The creation of BEV images is instrumental in providing a visual foundation for the scheduling system’s decision-making processes.

Following the generation of BEV images, the module undertakes the production of supplementary text. This text plays multiple roles, serving first as a SystemMessage that offers a deeper dive into the driving environment. It differentiates types of lane markings, delineates the driving layout, and categorizes vehicles into left-hand drive (LHD) and right-hand drive (RHD) based on their operational side and the side of the road they drive on. These objects are identified

by exclusive IDs, enabling the accuracy of textual expression for the LMM.

2) *Memory and Reflection Module*: As shown in the middle of Fig. 2, this module consists of two parts: the memory vectors and the reflection vectors. The memory module acts as a repository, storing historical images along with their corresponding textual information (i.e. prompting text and LMM response) in a stack. This stack is limited in size, ensuring that only the most recent and relevant information is retained for future reference.

Upon encountering collision cases, the reflection module feeds this multimodal data into the LMM for further analysis. The outcome of this reflection, alongside the original multimodal data, is stored back into the Memory module. This process enables the system to learn from past incidents and refine its decision-making capabilities over time.

3) *Retrieval Module*: The primary function of the retrieval module is to access the memory module for historical situations similar to the current context, thereby facilitating few-shot inference for scheduling decisions. By leveraging historical data, the system is capable of making informed, context-aware decisions that enhance both the efficiency and safety of the AMoD system’s operations. This module ensures that the LMM-based scheduling framework can adaptively respond to a diverse array of scenarios by drawing upon past experiences, thereby improving its management of the complex dynamics of urban traffic and AMoD system demands.

To facilitate the retrieval process, each BEV image in the Memory module is assigned an embedding using a pre-trained vision model. In this study, we adopt the Swin-Transformer [25], pre-trained on ImageNet-21k [26], owing to its superior capability in modeling multi-scale visual entities. This allows for the effective extraction of features

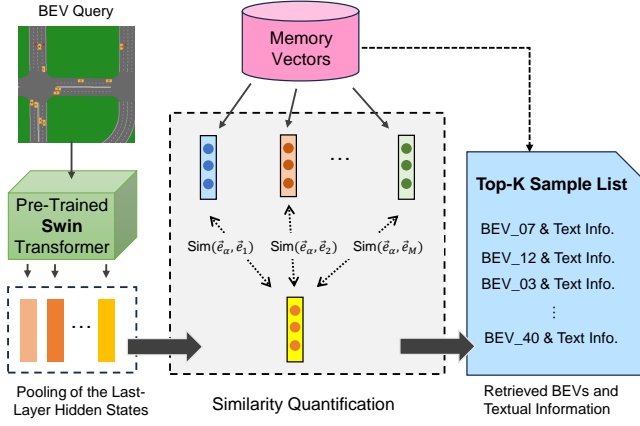


Fig. 3. Illustration of the retrieval for LMMCoDrive. A BEV image for similarity query is embedded with the pre-trained swin-transformer, before the pair-wise similarity quantification with the memory vectors. The memory samples of Top-K similarities are retrieved to support the online reasoning.

pertinent to both macroscopic traffic scenarios (such as intersections and multi-lane roadways) and microscopic object statuses (including vehicle IDs, positions, and orientations). The embedding is derived by average pooling of the final-layer hidden states to summarize the global feature representation. As illustrated in Fig. 3, during online retrieval, the real-time BEV image is first embedded using the vision model, and then its similarity to the memory samples is evaluated using the cosine similarity score:

$$\text{Sim}(\vec{e}_\alpha, \vec{e}_\beta) = \frac{\vec{e}_\alpha \cdot \vec{e}_\beta}{\|\vec{e}_\alpha\| \|\vec{e}_\beta\|}, \forall \beta \in \{1, 2, \dots, M\}, \quad (2)$$

where \vec{e}_α denotes the embedding of the newly generated BEV image used for the similarity query, while \vec{e}_β represents the embedding of any BEV image stored in the Memory module, and M indicates the size of the memory. Following this, the BEV images with the Top- K similarities are retrieved. This multimodal information forms the few-shot data that guide the online reasoning process.

B. LMM-Guided Cooperative Driving

For the scheduled AMoD vehicle fleet, we consider a cooperative motion planning task within subgraph \mathcal{H} generated by the LMM-guided graph evolution module. We formulate this task, involving N CAVs on urban roads with specified destinations and paths, as an OCP:

$$\begin{aligned} \min_{\mathbf{z}_\tau^i, \mathbf{u}_\tau^i} \quad & \sum_{i=1}^N Q_i(\mathbf{Z}^i, \mathbf{U}^i) \\ \text{s.t.} \quad & \mathbf{z}_{\tau+1}^i = f(\mathbf{z}_\tau^i, \mathbf{u}_\tau^i), \\ & \mathbf{z}_{\tau+1}^i \in \mathcal{S}_\tau^i, \\ & -\underline{\mathbf{u}}^i \leq \mathbf{u}_\tau^i \leq \bar{\mathbf{u}}^i, \\ & \forall \tau \in \mathcal{T}, \forall i \in \mathcal{N}, \end{aligned} \quad (3)$$

where \mathcal{N} represents the set of indices of CAVs within a subgraph \mathcal{H} , and $\mathcal{T} = \{0, 1, \dots, T-1\}$ denotes the temporal horizon for a cooperative motion planning episode. \mathcal{S}_τ^i defines the collision-free and bounded operational region for the i th CAV at time step τ . $\underline{\mathbf{u}}^i$ and $\bar{\mathbf{u}}^i$ represent the

Algorithm 1 Decentralized Optimization via Consensus ADMM in One Subgraph $\mathcal{H}(\mathcal{N}, \mathcal{E}_h)$

- 1: **initialize** $\{\mathbf{x}_\tau^i, \mathbf{u}_\tau^i\}_{\tau=0}^T, \{p^{i,0}, y^{i,0}, z^{i,0}, s^{i,0}\}, \forall i \in \mathcal{N}$
- 2: **choose** $\sigma, \rho > 0$
- 3: **repeat**:
- 4: Send $\{z_\tau^i\}_{\tau=1}^T$, receive $\{z_\tau^j\}_{\tau=1}^T$ from $j \in \mathcal{N}^i$
- 5: Compute $k^i, J^i, \{A_\tau^i\}_{\tau=0}^{T-1}, \{B_\tau^i\}_{\tau=0}^{T-1}$
- 6: **reset** $p^{i,0} = s^{i,0} = 0, y^{i,0} = y^{\text{last}}, x^{i,0} = x^{\text{last}}$
- 7: **reset** $y_{[2]}^{i,0} = x_{[2]}^{i,0} = 0$
- 8: **repeat**: for all $i \in \mathcal{N}$
- 9: Send $y^{i,k}$, receive $y^{j,k}$ from $j \in \mathcal{N}^i$
- 10: Broadcast $y^{i,k}$ to the vehicles in \mathcal{N}^i
- 11: $p^{i,k+1} = p^{i,k} + \rho \sum_{j \in \mathcal{N}^i} (y^{i,k} - y^{j,k})$
- 12: $s^{i,k+1} = s^{i,k} + \sigma (y^{i,k} - x^{i,k})$
- 13: $r^{i,k+1} = \sigma x^{i,k} + \rho \sum_{j \in \mathcal{N}^i} (y^{i,k} + y^{j,k}) - (k^i + p^{i,k+1} + s^{i,k+1})$
- 14: Perform (6a)-(6c) for $\alpha_{[2,i]}^{i,k}, \alpha \in \{p, s, r\}$
- 15: Perform (7a)-(7c) for $\alpha_{[2,j]}^{i,k}, \alpha \in \{p, s, r\}, j \in \mathcal{N}^i$
- 16: Compute $z^{i,k+1}$ by solving LQR problem (8)
- 17: $y_{[1]}^{i,k+1} = 2\gamma \left(\hat{J}^i z_{[1]}^{i,k+1} + r_{[1]}^{i,k+1} \right)$
- 18: $x_{[1]}^{i,k+1} = \Pi_{\mathcal{R}_+^c} \left(\frac{1}{\sigma} s_{[1]}^{i,k+1} + y_{[1]}^{i,k+1} \right)$
- 19: Perform (6d-6e) for $\alpha_{[2,i]}^{i,k}, \alpha \in \{y, x\}$
- 20: Perform (7d-7e) for $\alpha_{[2,j]}^{i,k}, \alpha \in \{y, x\}, j \in \mathcal{N}^i$
- 21: $k = k + 1$
- 22: **until** number of iteration steps exceeds k_{\max}
- 23: Update $\{z_\tau^i, \mathbf{u}_\tau^i\}_{\tau=0}^T$
- 24: **until** termination criterion is satisfied

lower and upper bounds of the control input for the i th CAV, respectively. The objective of this OCP is to enable the CAVs to follow their reference paths assigned by the upstream scheduling, which can be expressed as:

$$Q_i(z_\tau^i, \mathbf{u}_\tau^i) = \sum_{\tau=0}^T \|z_\tau^i - z_{\text{ref},\tau}^i\|_Q^2 + \sum_{\tau=0}^{T-1} \|\mathbf{u}_\tau^i\|_R^2, \quad (4)$$

where Q and R are the weighting matrices balancing the path tracking and energy saving.

1) *LMM-Guided Graph Evolution*: The graph evolution is essential for simplifying the OCPs involved in the motion planning of the CAV fleet. We employ a policy similar to that used in the scheduling process. However, the multimodal information integrator differs slightly from its scheduling counterpart. Since the graph evolution aims to identify groups of CAVs with potential collision risks, passenger requests are excluded from the BEV images, and the LMM's decision-making shifts from handling request-response pairs to identifying vehicle groups at risk of collision.

We generate a task description alongside retrieved similar multimodal contexts to form a few-shot example. Following the postprocessing of the LMM's output, the graph evolution, guided by the LLM, produces the groups of vehicles with collision risks. The corresponding adjacency matrix records the above information effectively, as depicted in Algorithm 2.

Algorithm 2 Cooperative Scheduling and Motion Planning for CAVs with LMM

- 1: **schedule** target positions of all CAVs in \mathcal{G} using LMM
 - 2: **determine** optimal route using A* for each CAV
 - 3: **smooth** the waypoints in each route by the Savitzky-Golay filter
 - 4: **while** \exists requests in the AMoD **do**:
 - 5: Execute LMM-guided graph evolution to distribute the CAVs to \mathcal{H}^k
 - 6: **for** subgraph \mathcal{H}^i in subgraphs list **do**
 - 7: **search** nearest waypoints for each CAV at each time step $\tau \in \{0, 1, \dots, T_s\}$ using KD-tree
 - 8: Execute Algorithm 1 to obtain CAVs' trajectories
 - 9: **end for**
 - 10: **perform** first T_e steps of the CAVs in \mathcal{G}
 - 11: **feedback** at time step T_e
 - 12: **relay** the states of all the CAVs in \mathcal{G}
 - 13: **end while**
-

2) *ADMM-Based Cooperative Motion Planning*: In order to reduce the size of the OCP and provide an agile response, MPC is used with a planning horizon $T_p = 15$, and an executing horizon $T_e = 10$. The dual formulation of the OCP derived from (3) is as follows:

$$\begin{aligned} \min_{\Delta \mathbf{Z}^1, \dots, \Delta \mathbf{Z}^N} \sum_{i=1}^N F^i(\Delta \mathbf{Z}^i) + \mathcal{I}_{\mathcal{K}}(\mathbf{h}) \\ \text{s.t. } \sum_{i=1}^N (\mathbf{J}^i \Delta \mathbf{Z}^i - \mathbf{k}^i) = \mathbf{h}, \end{aligned} \quad (5)$$

where $\Delta \mathbf{Z}^i$ is the concatenated vector of the state and control variables sequentially. F^i is the host cost for vehicle i , $\mathcal{I}_{\mathcal{K}}$ is the indicator function for the mutual avoidance and bounded constraints. More detailed information can be referred to in [27]. Leveraging the Lagrangian of (5), the problem is derived with the dual variables $\mathbf{p}, \mathbf{s}, \mathbf{r}, \mathbf{y}, \mathbf{x}$. *Dual update* is achieved by lines 10-15 and 17-20, while *primal update* is realized using line 16, as shown in Algorithm 1.

To enhance computational efficiency in the dual update process, we define two distinct sets of variables: one set associated with the target vehicle and another set pertaining to the surrounding vehicles that pose a collision risk to the target vehicle. We leverage (6) and (7) for the target vehicle and its surrounding connected vehicles, respectively.

$$\mathbf{p}_{[2,i]}^{i,k+1} = \mathbf{p}_{[2,i]}^{i,k} + \rho(N-1) \left(\mathbf{y}_{[2,i]}^{i,k} - \mathbf{y}_{[2,i]}^k \right), \quad (6a)$$

$$\mathbf{s}_{[2,i]}^{i,k+1} = \mathbf{s}_{[2,i]}^{i,k} + \sigma \left(\mathbf{y}_{[2,i]}^{i,k} - \mathbf{x}_{[2,i]}^{i,k} \right), \quad (6b)$$

$$\begin{aligned} \mathbf{r}_{[2,i]}^{i,k+1} = \sigma \mathbf{x}_{[2,i]}^{i,k} + \rho(N-1) \left(\mathbf{y}_{[2,i]}^{i,k} + \mathbf{y}_{[2,i]}^k \right) \\ - (\mathbf{k}_{[2,i]}^{i,k+1} + \mathbf{p}_{[2,i]}^{i,k+1} + \mathbf{s}_{[2,i]}^{i,k+1}), \end{aligned} \quad (6c)$$

$$\mathbf{y}_{[2,i]}^{i,k+1} = 2\gamma \left(\mathbf{O}^i \Delta \mathbf{Z}^{i,k+1} + \mathbf{r}_{[2,i]}^{i,k+1} \right), \quad (6d)$$

$$\mathbf{x}_{[2,i]}^{i,k+1} = \Pi_{\mathcal{S}^{b\circ}} \left(\frac{1}{\sigma} \left(\mathbf{s}_{[2,i]}^{i,k+1} + \mathbf{y}_{[2,i]}^{i,k+1} \right) \right). \quad (6e)$$

Note that for the dual update of $\mathbf{y}_{[2,i]}^{v,k+1}$ of the surrounding vehicles connected to the target vehicle, they only need to consider the consensus to $\mathbf{r}_{[2,i]}^{k+1}$ in (7d). For comparison, the target vehicle needs to consider the box constraints by calculating the high-dimensional matrix multiplication in (6d), which is time-consuming and meaningless.

$$\mathbf{p}_{[2,i]}^{v,k+1} = \mathbf{p}_{[2,i]}^k + \rho \left(\mathbf{y}_{[2,i]}^k - \mathbf{y}_{[2,i]}^{i,k} \right) = \mathbf{p}_{[2,i]}^{k+1}, \quad (7a)$$

$$\mathbf{s}_{[2,i]}^{v,k+1} = \mathbf{s}_{[2,i]}^k + \sigma \left(\mathbf{y}_{[2,i]}^k - \mathbf{x}_{[2,i]}^k \right) = \mathbf{s}_{[2,i]}^{k+1}, \quad (7b)$$

$$\begin{aligned} \mathbf{r}_{[2,i]}^{v,k+1} = \sigma \mathbf{x}_{[2,i]}^k + \rho(2|n^v| - 1) \mathbf{y}_{[2,i]}^k + \rho \mathbf{y}_{[2,i]}^{i,k} \\ - (\mathbf{k}_{[2,i]}^{k+1} + \mathbf{p}_{[2,i]}^{k+1} + \mathbf{s}_{[2,i]}^{k+1}) = \mathbf{r}_{[2,i]}^{k+1}, \end{aligned} \quad (7c)$$

$$\mathbf{y}_{[2,i]}^{v,k+1} = 2\gamma \mathbf{r}_{[2,i]}^{k+1} = \mathbf{y}_{[2,i]}^{k+1}, \quad (7d)$$

$$\mathbf{x}_{[2,i]}^{v,k+1} = \Pi_{\mathcal{S}^{b\circ}} \left(\frac{1}{\sigma} \left(\mathbf{s}_{[2,i]}^{k+1} + \mathbf{y}_{[2,i]}^{k+1} \right) \right) = \mathbf{x}_{[2,i]}^{k+1}, \quad (7e)$$

For the primal update process, due to the fully decentralized feature of the algorithm, only one target vehicle is considered in a standard LQR problem formulated as:

$$\begin{aligned} \min_{\Delta \mathbf{Z}^i} \Delta \mathbf{Z}^{i\top} \mathbf{L}_1^i + \frac{1}{2} \Delta \mathbf{Z}^{i\top} \mathbf{L}_2^i \Delta \mathbf{Z}^i + 2\mathbf{r}^{i,k+1\top} \mathbf{J}^i \Delta \mathbf{Z}^i \\ + \frac{1}{\sigma + 2\rho|n^i|} \Delta \mathbf{Z}^{i\top} \mathbf{J}^{i\top} \mathbf{J}^i \Delta \mathbf{Z}^i \\ \text{s.t. } (\mathbf{L}_3^i - \mathbf{L}_4^i) \Delta \mathbf{Z}^i = 0. \end{aligned} \quad (8)$$

Furthermore, as depicted in the Algorithm 2, in the scope of task execution, for the vehicles in the AMoD system, the vehicles need to evolve the connection graph guided by the LMM and solve the cooperative motion planning problems parallelly using the receding horizon manner.

V. SIMULATION RESULTS

A. Environment and Evaluation Metrics

We comprehensively evaluate the proposed LMMCoDrive framework in an AMoD system. For the scheduling and performance of the pairs of passengers and vehicles, we compare our proposed method with several popular heuristic algorithms, First Come First Serve (FCFS) and Distance First (DF). In terms of the graph evolution part for the vehicles, we execute an ablation study of our proposed method with the conditional Manhattan Distance-based method [24]. The out-of-box LMM is GPT-4o. All the experiments are executed in Town10HD of CARLA [28] with the assistance of LangChain in Python. The evaluation metrics are divided into two categories: scheduling and cooperative driving. For scheduling performance, we utilize the task completion time T_{tc} to assess the overall effectiveness of LMMCoDrive. Specifically, we calculate the average task completion time T_{atc} , the standard deviation T_{stc} , and the maximum task completion time T_{mtc} . The computational time for each episode of cooperative driving is utilized to represent the effectiveness of the LMM-guided graph evolution strategy.

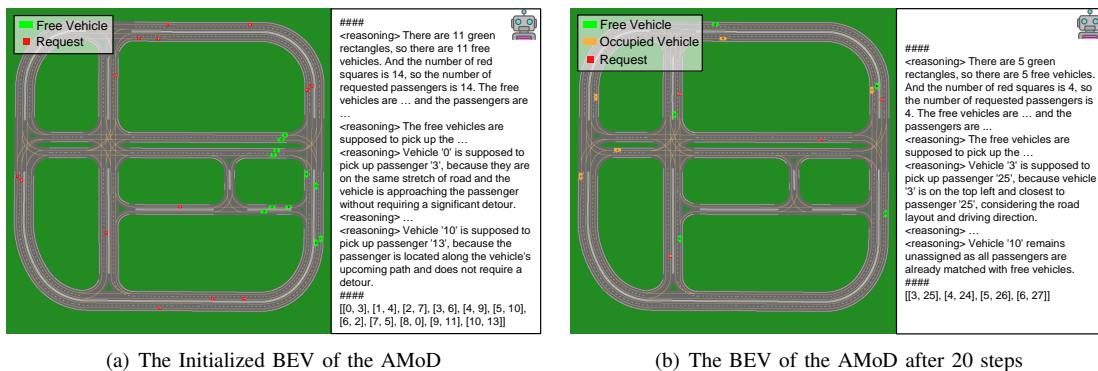


Fig. 4. The reasoning demonstration of the AMoD system utilizing our proposed LMMCoDrive framework: Green rectangles represent free vehicles, whereas yellow rectangles indicate vehicles occupied by passengers. Red squares signify pending requests from passengers within the AMoD system. The corresponding responses from the LMM are also revealed alongside the BEVs.

TABLE I
COMPARISON OF SCHEDULING EFFICIENCY BETWEEN LMMCoDRIVE AND TWO HEURISTIC ALGORITHMS

Method	Episode 1			Episode 2			Episode 3			Episode 4		
	T_{atc}	T_{stc}	T_{mtc}	T_{atc}	T_{stc}	T_{mtc}	T_{atc}	T_{stc}	T_{mtc}	T_{atc}	T_{stc}	T_{mtc}
FCFS	16.06	5.73	22.78	11.15	5.43	14.64	17.74	3.15	22.98	9.93	8.30	18.24
DF	10.72	6.69	22.97	4.81	5.66	14.61	5.83	4.05	12.31	9.93	8.30	18.24
LMMCoDrive	13.23	5.72	19.78	3.49	3.95	10.34	13.46	3.17	18.23	8.42	7.06	15.48

B. Scheduling Performance

We conduct the comparisons in the aforementioned AMoD system with 10 CAVs, and requests from passengers from all over the traffic system are gradually raised. As shown in Fig. 4, the vehicles convey passengers to their randomly generated destinations with the yellow remark. As for the free vehicles, once they are assigned a passenger in the AMoD system, they will drive to their customs and serve them as soon as possible. As depicted in Table I, in most cases, LMMCoDrive has the smallest T_{mtc} and T_{stc} , while maintaining good T_{atc} . It proves the excellent scheduling performance for the AMoD. The LMMCoDrive achieves a balance between efficiency and passenger experience, but performs unstable in some cases, and this indicates that the prompt of the LMM can be further refined.

C. Ablation Study

The purpose of this ablation study is to evaluate the effectiveness of the LMM in the graph evolution process for AMoD systems. By default, the graph evolution setting employs a heuristic strategy similar to those detailed in Section V-B. As illustrated in Fig. 5, the LMM's capability to accurately and flexibly determine groups of CAVs with collision risks results in a significantly lower average computation time for parallel OCPs compared to the Manhattan distance-based graph-evolution method. The primary reason for this improvement is that LMMCoDrive can more precisely identify potential collisions, thereby avoiding overly conservative decisions that would otherwise increase the number of CAVs in one OCP leading to computational overhead.

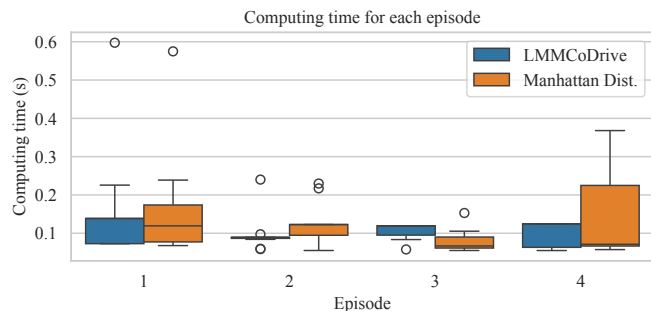


Fig. 5. The computation time for each episode of the receding horizon for cooperative motion planning. For the first column of boxes, the graph of the connection of the vehicles is evolved by LMM, while the second column is the result of the Manhattan distance-based heuristic method.

VI. CONCLUSION

In this paper, we propose LMMCoDrive, an LMM-enabled integrated scheduling and cooperative motion planning framework suitable for AMoD systems in urban scenarios. The incorporation of a BEV that describes the traffic situation expands the boundary of the applications of LLMs, and this alleviates the travel prompt engineering. Simulation results demonstrate LMM's role in optimizing CAV scheduling and facilitating decentralized cooperative optimization. It's a significant milestone towards practical and efficient AMoD systems, which also offers insights for future urban transportation solutions. Future work will focus on further refining its information flow to achieve a more robust performance and expanding its application to larger and more complex urban cooperative driving scenarios.

REFERENCES

- [1] S. Hörll, M. Balac, and K. W. Axhausen, "Dynamic demand estimation for an AMoD system in paris," in *the Proceedings of 2019 IEEE Intelligent Vehicles Symposium*, 2019, pp. 260–266.
- [2] X. Ding, Q. Qi, S. Jian, and H. Yang, "Mechanism design for mobility-as-a-service platform considering travelers' strategic behavior and multidimensional requirements," *Transportation Research Part B: Methodological*, vol. 173, pp. 1–30, 2023.
- [3] A. Aalipour and A. Khani, "Modeling, analysis, and control of autonomous mobility-on-demand systems: A discrete-time linear dynamical system and a model predictive control approach," *IEEE Transactions on Intelligent Transportation Systems*, 2024.
- [4] F. Javanshour, H. Dia, G. Duncan, R. Abduljabbar, and S. Liyanage, "Performance evaluation of station-based autonomous on-demand car-sharing systems," *IEEE Transactions on Intelligent Transportation Systems*, vol. 23, no. 7, pp. 7721–7732, 2021.
- [5] M. Veres and M. Moussa, "Deep learning for intelligent transportation systems: A survey of emerging trends," *IEEE Transactions on Intelligent transportation systems*, vol. 21, no. 8, pp. 3152–3168, 2019.
- [6] J. Karlsson, C.-I. Vasile, J. Tumova, S. Karaman, and D. Rus, "Multi-vehicle motion planning for social optimal mobility-on-demand," in *the Proceedings of 2018 IEEE International Conference on Robotics and Automation*, 2018, pp. 7298–7305.
- [7] T. Enders, J. Harrison, M. Pavone, and M. Schiffer, "Hybrid multi-agent deep reinforcement learning for autonomous mobility on demand systems," in *the Proceedings of Learning for Dynamics and Control Conference*, 2023, pp. 1284–1296.
- [8] S. He, Y. Wang, S. Han, S. Zou, and F. Miao, "A robust and constrained multi-agent reinforcement learning electric vehicle rebalancing method in amod systems," in *the Proceedings of 2023 IEEE/RSJ International Conference on Intelligent Robots and Systems*, 2023, pp. 5637–5644.
- [9] F. Dandl, R. Engelhardt, M. Hyland, G. Tilg, K. Bogenberger, and H. S. Mahmassani, "Regulating mobility-on-demand services: Tri-level model and bayesian optimization solution approach," *Transportation Research Part C: Emerging Technologies*, vol. 125, p. 103075, 2021.
- [10] G. Guo and Y. Hou, "Rebalancing of one-way car-sharing systems considering elastic demand and waiting time," *IEEE Transactions on Intelligent Transportation Systems*, vol. 23, no. 12, pp. 23 295–23 310, 2022.
- [11] J. Wei, X. Wang, D. Schuurmans, M. Bosma, F. Xia, E. Chi, Q. V. Le, D. Zhou *et al.*, "Chain-of-thought prompting elicits reasoning in large language models," *Advances in neural information processing systems*, vol. 35, pp. 24 824–24 837, 2022.
- [12] W. Huang, C. Wang, R. Zhang, Y. Li, J. Wu, and L. Fei-Fei, "Voxposer: Composable 3d value maps for robotic manipulation with language models," in *the Proceedings of Conference on Robot Learning*, 2023, pp. 540–562.
- [13] W. Zu, W. Song, R. Chen, Z. Guo, F. Sun, Z. Tian, W. Pan, and J. Wang, "Language and sketching: An llm-driven interactive multimodal multitask robot navigation framework," in *the Proceedings of 2024 IEEE International Conference on Robotics and Automation*, 2024, pp. 1019–1025.
- [14] S. Yao, D. Yu, J. Zhao, I. Shafran, T. Griffiths, Y. Cao, and K. Narasimhan, "Tree of thoughts: Deliberate problem solving with large language models," *Advances in Neural Information Processing Systems*, vol. 36, 2024.
- [15] L. Wen, D. Fu, X. Li, X. Cai, T. Ma, P. Cai, M. Dou, B. Shi, L. He, and Y. Qiao, "Dilu: A knowledge-driven approach to autonomous driving with large language models," *arXiv preprint arXiv:2309.16292*, 2023.
- [16] C. Cui, Y. Ma, X. Cao, W. Ye, Y. Zhou, K. Liang, J. Chen, J. Lu, Z. Yang, K.-D. Liao *et al.*, "A survey on multimodal large language models for autonomous driving," in *the Proceedings of the IEEE/CVF Winter Conference on Applications of Computer Vision*, 2024, pp. 958–979.
- [17] B. Li, T. Acarman, Y. Zhang, Y. Ouyang, C. Yaman, Q. Kong, X. Zhong, and X. Peng, "Optimization-based trajectory planning for autonomous parking with irregularly placed obstacles: A lightweight iterative framework," *IEEE Transactions on Intelligent Transportation Systems*, vol. 23, no. 8, pp. 11 970–11 981, 2022.
- [18] Z. Huang, H. Liu, S. Shen, and J. Ma, "Parallel optimization with hard safety constraints for cooperative planning of connected autonomous vehicles," in *the Proceedings of 2024 IEEE International Conference on Robotics and Automation*, 2024, pp. 2238–2244.
- [19] Y. Lee, M. Cho, and K.-S. Kim, "GPU-parallelized iterative LQR with input constraints for fast collision avoidance of autonomous vehicles," in *the Proceedings of 2022 IEEE/RSJ International Conference on Intelligent Robots and Systems*, 2022, pp. 4797–4804.
- [20] J. Ma, Z. Cheng, X. Zhang, M. Tomizuka, and T. H. Lee, "Alternating direction method of multipliers for constrained iterative LQR in autonomous driving," *IEEE Transactions on Intelligent Transportation Systems*, vol. 23, no. 12, pp. 23 031–23 042, 2022.
- [21] J. Chen, W. Zhan, and M. Tomizuka, "Autonomous driving motion planning with constrained iterative LQR," *IEEE Transactions on Intelligent Vehicles*, vol. 4, no. 2, pp. 244–254, 2019.
- [22] J. Ma, Z. Cheng, X. Zhang, Z. Lin, F. L. Lewis, and T. H. Lee, "Local learning enabled iterative linear quadratic regulator for constrained trajectory planning," *IEEE Transactions on Neural Networks and Learning Systems*, vol. 34, no. 9, pp. 5354–5365, 2023.
- [23] Z. Huang, S. Shen, and J. Ma, "Decentralized iLQR for cooperative trajectory planning of connected autonomous vehicles via dual consensus ADMM," *IEEE Transactions on Intelligent Transportation Systems*, 2023.
- [24] H. Liu, Z. Huang, Z. Zhu, Y. Li, S. Shen, and J. Ma, "Improved consensus admm for cooperative motion planning of large-scale connected autonomous vehicles with limited communication," *IEEE Transactions on Intelligent Vehicles*, pp. 1–17, 2024.
- [25] Z. Liu, Y. Lin, Y. Cao, H. Hu, Y. Wei, Z. Zhang, S. Lin, and B. Guo, "Swin transformer: Hierarchical vision transformer using shifted windows," in *the Proceedings of the IEEE/CVF international conference on computer vision*, 2021, pp. 10 012–10 022.
- [26] J. Deng, W. Dong, R. Socher, L.-J. Li, K. Li, and L. Fei-Fei, "Imagenet: A large-scale hierarchical image database," in *the Proceedings of 2009 IEEE conference on computer vision and pattern recognition*, 2009, pp. 248–255.
- [27] P. D. Grontas, M. W. Fisher, and F. Dörfler, "Distributed and constrained H_2 control design via system level synthesis and dual consensus ADMM," in *the Proceedings of 2022 IEEE 61st Conference on Decision and Control*, 2022, pp. 301–307.
- [28] A. Dosovitskiy, G. Ros, F. Codevilla, A. Lopez, and V. Koltun, "CARLA: An open urban driving simulator," in *the Proceedings of Conference on Robot Learning*, 2017, pp. 1–16.